

# Complexation between porcine gastric mucin (PGM) and lysozyme: Influence of heat treatment of lysozyme on the tribological properties

**Shirazi, Hadi Asgharzadeh; Lee, Seunghwan**

*Published in:*
International Journal of Biological Macromolecules

*Link to article, DOI:*
10.1016/j.ijbiomac.2022.01.122

*Publication date:*
2022

*Document Version*
Peer reviewed version

Journal Pre-proof


# Complexation between porcine gastric mucin (PGM) and lysozyme: Influence of heat treatment of lysozyme on the tribological properties

Hadi Asgharzadeh Shirazi, Seunghwan Lee

PII: S0141-8130(22)00137-4

DOI: https://doi.org/10.1016/j.ijbiomac.2022.01.122

Reference: BIOMAC 20274

To appear in: *International Journal of Biological Macromolecules*

Received date: 10 November 2021

Revised date: 12 January 2022

Accepted date: 19 January 2022

Please cite this article as: H.A. Shirazi and S. Lee, Complexation between porcine gastric mucin (PGM) and lysozyme: Influence of heat treatment of lysozyme on the tribological properties, *International Journal of Biological Macromolecules* (2021), https://doi.org/10.1016/j.ijbiomac.2022.01.122

# Complexation between porcine gastric mucin (PGM) and lysozyme: Influence of heat treatment of lysozyme on the tribological properties

Hadi Asgharzadeh Shirazi*, Seunghwan Lee

Department of Mechanical Engineering, Technical University of Denmark, DK-2800, Kgs. Lyngby, Denmark

*Corresponding author. E-mail address: shirazifard.hadi@gmail.com

## Abstract

The influence of complexation between porcine gastric mucin (PGM) and lysozyme (LYZ) solutions (pH~7.0) on their lubricating properties was studied at a hydrophobic self-mated polydimethylsiloxane (PDMS) tribopair. To this end, LYZ solutions with varying heating time, namely $1^{hr}$, $3^{hr}$-, and $6^{hr}$ at 90°C, as well as unheated LYZ solution, were prepared. The lubricating capability of PGM and LYZ solutions and also their mixtures was characterized using pin-on-disk tribometry. In parallel, to precisely investigate the interaction between PGM and LYZ solutions, an array of the well-known experiments including electrophoretic-dynamic light scattering, circular dichroism spectroscopy and optical waveguide light-mode spectroscopy were employed. These experiments were utilized to elucidate the key features e.g. zeta potential, hydrodynamic diameter, conformational structure and mass adsorption. The tribometry results indicated that both PGM and unheated LYZ solutions had poor lubricating properties in the boundary lubrication regime (sliding speed lower than 10 mm/s). Mixing PGM with unheated LYZ led to a slight decrease in the friction coefficient, but no desirable lubricity was observed. An optimum slippery characteristic was achieved by incorporating $1^{hr}$ heated LYZ solution into PGM one. Excellent lubricity of PGM/$1^{hr}$ heated LYZ may stem from surface charge compensation, tenaciously compact aggregation, unique conformational structure and considerable mass adsorption onto PDMS. This finding revealed that a strong interaction between PGM and LYZ molecules and as a result, the promising lubricating capability of PGM/LYZ mixtures, can be administered by varying heat-treatment duration of LYZ proteins.

**Keywords:** Porcine gastric mucin (PGM); Lysozyme; Synergistic lubrication; Structural and physicochemical characterizations.

## 1. Introduction

Biological lubricants play a vital role to minimize wear and dissipation of energy in living organisms and bio-devices. Mucus is one of the most well-known biological lubricants that can be found plentifully in the nature of the human body e.g. tear film, saliva, respiratory, reproductive and gastrointestinal tracts [1]. Mucus is primarily composed of water, electrolytes and mucins [2]. Mucin, the key component bringing excellent lubricating and protective properties of mucus, is a glycoprotein consisting of linear polypeptide backbone and covalently linked oligosaccharide side-chains [3]. An important structural feature of mucin is its distinct amphiphilicity; the central region of the backbone is heavily glycosylated (and thus hydrophilic), whereas the C- and N-termini are largely unglycosylated (and thus hydrophobic) [4]. A number of interesting phenomena, such as improving water wettability of polymeric substrates [5], ability to bind to bacteria [6], and aqueous lubrication [7], are derived from mucin's amphiphilicity.

Recently, the lubricating properties of mucin have received considerable attention, in particular, due to its lubricity in the aqueous environment and a consequent potential of application in bioengineering [8]. Hydrophobic patches of end groups of mucins function as anchors onto the substrate, and the central hydrophilic patches function to attract water as a base lubricant at the polymer/water interface. However, this simple view holds true only for certain types of mucins, e.g. bovine submaxillary mucin (BSM) [9] or purified intestinal mucins [10], whereas other types, for example, commercially available porcine gastric mucin (PGM) does not display an effective aqueous lubrication on its own [9,10]. It should be stressed though that as the amount of adsorption of PGM (e.g. areal mass of the spontaneously adsorbed film) onto a hydrophobic surface is typically higher than that of BSM [9], poor lubricity of PGM should be ascribed to other reasons than poor surface adsorption, such as the formation of relatively weak films to withstand tribological stress [9]. Even though the lubricating properties of PGM are improved to a certain extent by exposing to an acidic environment [11], being slippery at neutral aqueous conditions would be more desirable and promising for even broader range of bioengineering applications.

As one way to compensate for this drawback as a lubricant additive, several polycations have been employed as 'artificial crosslinkers' including polyallylamine hydrochloride (PAH) [12],

poly-l-lysine (PLL) [12], polyethylenimine (PEI) [12] (both linear and branched) [12,13] and chitosan [14]. These studies indicated that neither PG mucin nor polycations could have slippery characteristics alone, but the lubricating properties of PGM (or synergistic lubricating behavior) were greatly enhanced by mixing with such polycations [12-14]; the coefficient of friction is on the level of 0.02 at the lowest speed of 0.25 mm/s, which is comparable to the best performance of BSM [9]. In a way, the cationic crosslinkers appear to play a similar role of protons ($H^+$) when PGM shows improved lubricating properties at acidic pH [11]. A strong electrostatic attraction and complexation between negatively charged PGM and positively charged polycations was described as one of the key factors to drive a significant improvement in lubricating properties of mucins [12-14].

Given that various polycations serve as effective 'artificial' crosslinkers between PGMs, it is of curiosity whether other cationic entities may display similar behavior. In particular, small proteins with isoelectric point (IEP) higher than 7 should be similar to synthetic polycations mentioned above in size, conformation, and electrostatic properties, and are outstanding candidates to compare. In this context, lysozyme (LYZ) is a common and representative protein that exhibits distinctly positive charge characteristics in neutral pH with its IEP at ~11 [15]. Lysozyme (LYZ) is an antimicrobial protein and has a marked tendency to bind with negatively charged biological materials like mucin (e.g. ovomucin in egg white) [16]. Moreover, the structure of LYZ in an aqueous solution can be varied by ambient condition, especially by temperature [17-20], while preserving all the chemical identities. For this reason, heat treatment of LYZ is expected to provide a unique opportunity to investigate the influence of conformational changes of polycation on the complexation with PGM as well as the synergistic lubricating effects.

## 2. Materials and methods

### *2.1.Chemicals*

PGM (Mucin from the porcine stomach, Type III, bound sialic acid 0.5-1.5 %, partially purified powder) and lysozyme (from chicken egg white, dialyzed, lyophilized, powder, ~100000 U/mg) were purchased from Sigma-Aldrich (Brøndby, Denmark). Firstly, stock solutions of PGM and lysozyme (LYZ) were prepared at a concentration of 1 mg/mL in 4-(2-Hydroxyethyl)piperazine-1-ethanesulfonic acid (HEPES) buffer (1 mM, pH 7 as adjusted by

addition of NaOH). For heat-treatment of lysozyme, LYZ solutions were transferred into glass test tubes and heated in a water bath at 90 °C for 0, 1, 3 and 6 hours, respectively. Then, all heated LYZ solutions were allowed to cool down to room temperature (ca. 25 °C). In contrast, PGM solutions were not subjected to heat treatment. Afterwards, each of LYZ solutions was mixed with PGM solution to prepare PGM:LYZ mixture solutions at 1:1 (v:v) ratio. The concentration of PGM, LYZ, and PGM/LYZ mixtures was fixed at 1mg/mL in this study.

### *2.2.Pin-on-disk tribometry*

The friction coefficient ($\mu$, defined as the ratio between friction force ($F_{\text{Friction}}$)/normal force ($F_{\text{Normal}}$)) of PGM, unheated/heated LYZ, and their mixture solutions were determined by means of a pin-on-disk tribometer (CMS, Peseux, Switzerland) with accompanying software (Version 4.4.M, InstrumX). In this approach, a loaded pin was allowed to have contact with a disk, placed in a cell containing liquid medium (tribocup), and to rotate on a fixed track of disk (radius of 4 mm). The sliding friction forces between the pin and the disk were measured using a strain gauge at a controlled rotation speed of the disk. In this study, the normal load applied by dead weight on the pin was fixed at 1 N to provide mild mechanical stress. The range of sliding speed was varied from 0.25 to 100 mm/s, and then $\mu$ values were acquired at each speed. The lubricating properties of sample solutions were assessed by comparing $\mu$ vs. speed plots of sample solutions and HEPES buffer as a reference.

Polydimethylsiloxane (PDMS) was employed as materials for both pin and disk. To prepare a self-mated PDMS tribopair for pin-on-disk tribometry experiment, PDMS pins and disks were fabricated using the commercial base fluid and crosslinker (curing agent) of a Sylgard 184 elastomer kit (Dow Corning, Midland, MI). Base fluid and crosslinker were thoroughly mixed at a weight ratio of 10:1. Generated air bubbles were removed via a gentle vacuum. The obtained fluid mixture was gently poured into a commercial polystyrene cell culture plate with round-shaped wells (3 mm radius, 96 MicroWell Plates, NUNCLON Delta Surface, Roskilde, Denmark) and a machined aluminum plate mold with flat wells (30 mm diameter × 5 mm thickness) to fabricate the pin and the disk shapes of tribopair, respectively. PDMS specimens were allowed to cure at 70 °C overnight. The elastic modulus and Poisson's ratio of PDMS prepared according to this protocol are expected to be ca. 2 MPa and 0.5, respectively [11].

### *2.3.Optical waveguide light-mode spectroscopy (OWLS)*

The absorbed masses of selected proteins onto PDMS surfaces were measured using an OWLS 210 label-free Biosensor system (Microvacuum LTD, Budapest, Hungary). OWLS is an effective technique to monitor the adsorption of macromolecules on a surface created on a sensor. In this configuration, a grating assists with the in-coupling of light (He–Ne laser) into a planar optical waveguide coating (a 200 nm thick $Si_{0.25}Ti_{0.75}O_2$ waveguiding layer on 1 mm thick AF 45 glass, Microvacuum Ltd, Budapest, Hungary) to measure the mass adsorption. In order to obtain the absorbed masses on the PDMS surfaces, the waveguides were spin-coated with an ultrathin layer of PDMS at 2000 rpm for 25 s. Prior to the PDMS coating, an ultrathin layer (~30 nm) of PS (polystyrene, Sigma Aldrich, Brøndby, Denmark) was spin-covered on waveguides at 2500 rpm for 15 s to avoid likely chemical bonding of PDMS with $Si_{0.25}Ti_{0.75}O_2$ waveguiding layer. The intermediate PS layer is helpful in removing PDMS after measurements. To this end, PS was prepared at a concentration of 6 mg/ml in toluene. Moreover, the base and curing agents of the silicone elastomer (Sylgard 184 elastomer kit, Dow Corning, Midland, MI) were dissolved in hexane at a ratio of 10:3 (final concentration, 0.5% w/w) to obtain PDMS solution. All PS/PDMS spin-coated waveguides were cured at 70°C overnight.

During OWLS experiments, the cured PS/PDMS waveguides were placed into a flow-cell holder in the device based on manufacturing instruction. The surface of the waveguide was exposed to a constant HEPES buffer flow using a programmable syringe pump (Model AL-1000, World Precision Instruments, Florida). This process was continued until a stable baseline was reached. Subsequently, 100 µl of the solution was injected into the surface via a loading loop. The pump flow was stopped upon any change in the surface adsorption was observed. After 15 min, the HEPES flow was re-circuited to rinse the flow-cell including loosely bound macromolecules from the waveguiding surface. The adsorbed mass densities were calculated according to Feijter's equation as $M = d_A \frac{n_A - n_c}{{d_n}/{d_c}}$ [21]. $d_A$ is the thickness of the adsorbed layer and $d_n/d_c$ denotes the refractive index increment of the molecules. $n_A$ and $n_c$ are refractive indices of the adsorbed molecules and the cover medium. OWLS technique is sensitive to changes in the refractive index [22], therefore the refractive indices of the solutions were determined experimentally using an automatic refractometer (J157, Rudolph), averaged by ten measurements. OWLS experiments were repeated at least three times for each solution and all the measurements were performed using the Biosense 2.6.10 software.

### *2.4.Zeta potentials (ζ)*

Zeta potentials (ζ) of the sample solutions were assessed using a Zetasizer NANO instrument (Model ZEN5600, Malvern Instruments Ltd., UK) and its analyzer software (Zetasizer 7.11). Disposable folded capillary cells (Model DTS1070, Malvern Instruments Ltd., UK) were employed to add solutions to the apparatus. Before the test, the disposable cells and the electrodes were carefully cleaned with Millipore water and ethanol in sequence, and then blown-dried with nitrogen. Three measurements were carried out for statistical evaluation where each measurement was the average of ten repeats.

### *2.5.Dynamic light scattering (DLS)*

DLS was performed on each sample solution with a Zetasizer NANO instrument (Model ZEN5600, Malvern Instruments Ltd., UK) based on phase analysis light scattering with particle/molecule sizing software (Zetasizer 7.11). Disposable cuvettes (VMR® Semi-micro Polystyrene (PS) Cuvettes) were carefully cleaned with Millipore water and ethanol in sequence, and blown-dried with nitrogen. The DLS instrument analyzed each solution for at least five runs and each run consisted of ten averaged measurements.

### *2.6.Circular dichroism (CD) spectroscopy*

CD spectroscopy was performed to characterize the conformational features of proteins in the solutions by acquiring far-ultraviolet (FUV) CD spectra (from 280 to 190 nm) and near UV (NUV) CD spectra (from 400 to 250 nm) with a step size of 1 nm and a bandwidth of 1 nm. Rectangular quartz cuvettes (Hellma GmbH & Co.KG, Mulheim, Germany) with a path length of 0.5 mm (for far UV) and a 10 mm (for near UV) were used to place into a Chirascan spectrophotometer (Applied Photophysics Ltd, Surrey, UK). The measurements were performed at room temperature (ca. 25°C), and the data were averaged of two independent measurements for both FUV and NUV CD spectra. Each measurement was obtained from averaging three traces.

## 3. **Results**

### *3.1.Tribological properties: pin-on-disk tribometry*

Figure 1 displays the changes in the friction coefficient ($\mu$) of HEPES buffer, PGM, unheated LYZ, PGM/unheated LYZ, PGM/1$^{hr}$ heated LYZ, PGM/3$^{hr}$ heated LYZ, and PGM/6$^{hr}$ heated LYZ in the variation of the sliding speed from 0.25 mm/s to 100 mm/s.

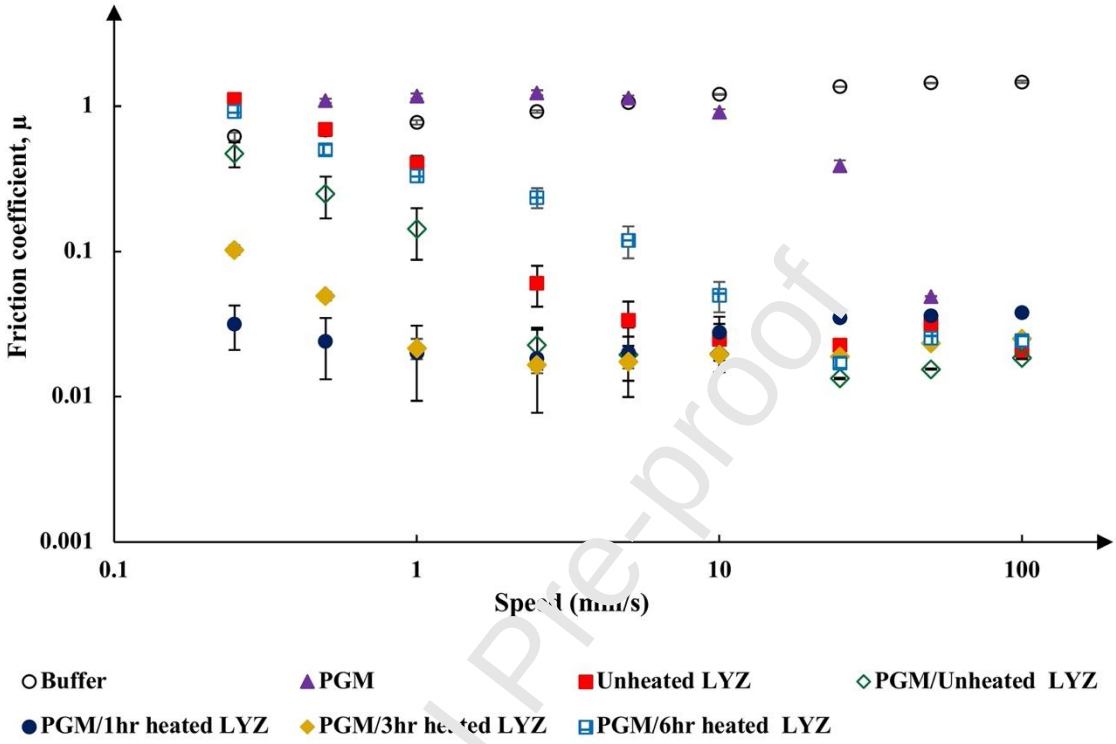


**Figure 1.** Influence of HEPES buffer, PGM, un-/heat-treated LYZ, and PGM/LYZ mixture solutions as lubricants on the friction coefficient of PDMS-PDMS pin-on-disk pairs in response to different sliding speeds in the range of 0.25-100 mm/s.

Apart from buffer and PGM, all solutions showed low values of $\mu$ ($\leq$ 0.05) at speeds $\geq$ 10 mm/s. Meanwhile, in the low-speed regime (< 10 mm/s), the sample solutions showed large differences from each other in the $\mu$ values.

First of all, PGM exhibited a negligible improvement in the lubricating properties compared to buffer except in the very high-speed regime ($\geq$ 50 mm/s), which is in line with the studies reported in the literature [11-14]. The $\mu$ values of unheated LYZ in high-speed regime ($\geq$ 10 mm/s) are also very low (ca. 0.03), but started to increase rapidly with decreasing speed, reaching $\mu \approx 1.11$ at the lowest speed (0.25 mm/s). Despite a clear difference in the transition threshold speeds, both PGM and unheated LYZ showed a similar trend in the lubricating properties, i.e. low $\mu$ values in the high-speed regime, followed by a drastic increase in $\mu$ values in the low-speed regime. Most importantly, neither PGM nor LYZ evinced an effective boundary

lubricating behavior in a low-speed regime. Meanwhile, all the mixture solutions of PGM and LYZ showed a synergistic effect in the boundary lubricating properties in that the $\mu$ values were clearly lower than those of PGM or LYZ alone. This means that LYZ may function as an artificial crosslinker similar to synthetic polymers in previous studies [12-14]. However, the extent of synergistic lubrication was highly dependent on the heating duration of LYZ, and the $\mu$ values were ranked in the order of PGM/$1^{hr}$ heated LYZ < PGM/$3^{hr}$ heated LYZ < PGM/unheated LYZ ≈ PGM/$6^{hr}$ heated LYZ. PGM/$3^{hr}$ heated LYZ pair manifested similarly low $\mu$ values with PGM/$1^{hr}$ heated LYZ down to 1 mm/s, but somewhat higher values at lower speeds. In comparison with the previously studied lubrication between PGM and synthetic polycations, e.g. PGM/chitosan (under acidic conditions) and PGM/b-PEI [12-14], PGM/$1^{hr}$ heated LYZ pair is the only one that showed a comparably effective lubricating effect down to the lowest speed ($\mu$ = 0.03 at 0.25 mm/s).

### *3.2.Surface adsorption of PGM, un-/$1^{hr}$ heat-treated LYZ and their mixtures: OWLS experiments*

A substantial increase in the adsorbed mass of the mixture onto tribopair (PDMS) surface compared to those of PGM or polycation alone is one of the characteristic features of PGM-polycation mixtures, showing a synergistic lubricating effect [12-14]. This was attributed to more favorable adsorption of less charged species, i.e. PGM-polycation mixture, onto the nonpolar surface of PDMS compared to distinctly charged PGM (negatively) or polycations (positively). To examine whether this effect is observable from PGM and LYZ systems too, PGM/unheated LYZ and PGM/$1^{hr}$ heated LYZ were selected as representative examples showing an ineffective and an effective synergistic lubricity upon mixing with PGM, respectively (Figure 1), and the areal adsorbed masses of were determined by means of OWLS. The adsorbed mass values of PGM, un-/$1^{hr}$ heat-treated LYZ and their mixture solutions onto PDMS are shown in Figure 2. The concentration dependence of the refractive index of each solution, $dn/dc$, which is necessary to estimate the areal mass according to Feijter's equation, was experimentally determined and is presented in Table 1.

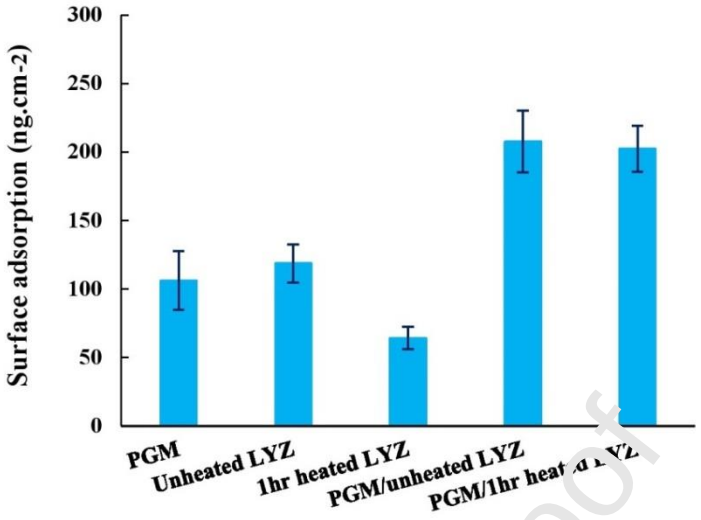


**Figure 2.** Surface adsorbed mass values of PGM, unheated LYZ, $1^{hr}$ heated LYZ and the mixture solutions of PGM/unheated LYZ and PGM/$1^{hr}$ heated LYZ onto PDMS-coated waveguides measured by OWLS. The adsorption time was 15 min.

**Table 1.** Refractive index (dn/dc) values for PGM, unheated/$1^{hr}$ heat-treated LYZ and their mixture solutions in order to employ in the mass adsorption calculations during OWLS experiment.

| **Solution** | PGM | Unheated LYZ | $1^{hr}$ heated LYZ | PGM/unheated LYZ | PGM/$1^{hr}$ heated LYZ |
|---|---|---|---|---|---|
| **dn/dc ($cm^3/g$)** | 0.120 | 0.184 | 0.234 | 0.114 | 0.153 |

PGM and unheated LYZ displayed the areal mass values of 106.2 ± 21.5 and 118.7 ± 14.0 $ng/cm^2$, respectively. The value for PGM has a good agreement with those in previous studies [12-14]. Mixing PGM with either unheated or $1^{hr}$ heated LYZ led to a considerable increase in the adsorbed mass compared to PGM and LYZ alone; 207.5 ± 22.6 $ng/cm^2$ for PGM/unheated LYZ mixture and 202.2 ± 16.8 $ng/cm^2$ for PGM/$1^{hr}$ heated LYZ mixture, respectively. As mentioned above, neutralization of surface charges of PGM and LYZ is likely to be the reason for the increased amount of adsorption on the nonpolar PDMS surface for PGM/LYZ mixtures, similarly with the cases of PGM/b-PEI [12,13] and PGM/chitosan [14]. An important point to note though is that not only PGM/$1^{hr}$ heated LYZ mixture, but also PGM/unheated LYZ mixture showed a substantial increase in the areal adsorbed mass, despite the lack of an effective synergistic lubrication for the latter (Figure 1).

### *3.3.ζ potential measurements: Electrophoretic light scattering (ELS)*

Given that the interaction between PGM and LYZ is driven primarily by an electrostatic attraction, zeta (ζ) potentials of PGM, LYZ, and their mixtures may provide an insight into the characteristics of interaction between them. The ζ values of PGM, un-/heat-treated LYZ and their mixture solutions are plotted in Figure 3.

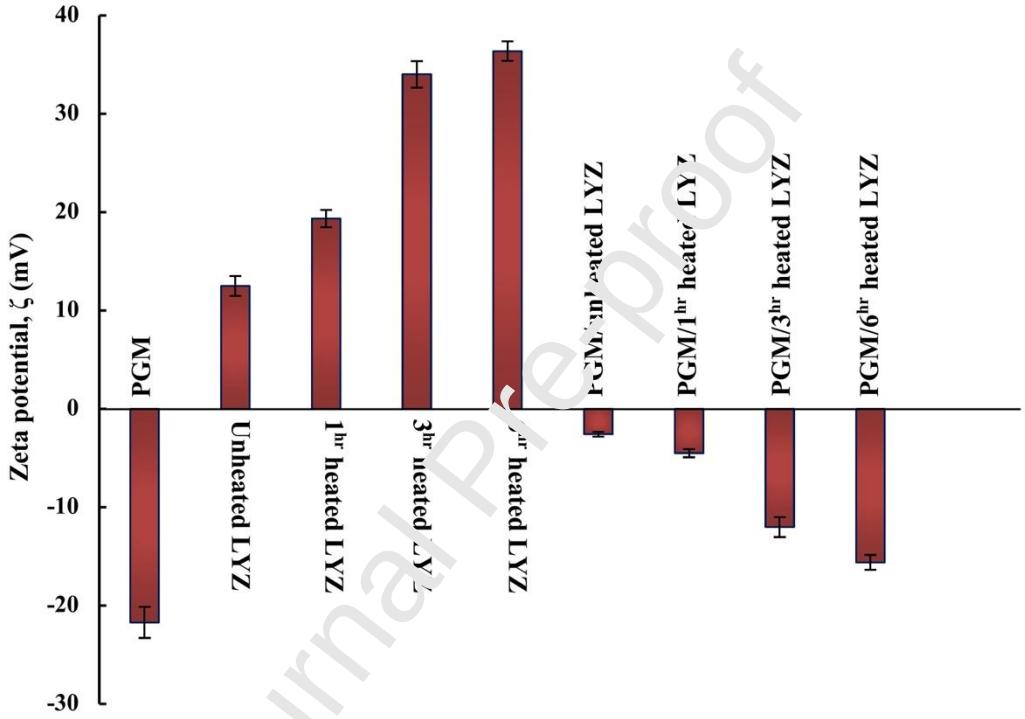


**Figure 3.** Zeta (ζ) potential values of PGM, un-/heat-treated LYZ, and their mixtures. By increasing the heating time of LYZ, ζ potential of LYZ shifts toward more positive values whereas ζ potential of PGM/LYZ mixture gradually shifts from neutral to negative direction.

Clearly, PGM and LYZ solutions showed high negative and positive ζ potentials of -21.7 ± 1.6 and 12.5 ± 1.0 mV, respectively. PGM contains negatively charged moieties, mostly in sugar chains in the central domain [23,24]. LYZ possesses a large number of $-NH_2$ groups [25], and it can explain a positive surface charge at pH∼7. The ζ potential values observed in this study were slightly higher for the case of PGM [12,13] and very similar for the case of LYZ [26,27] compared to those reported in previous studies.

As shown in Figure 3, heat treatment on LYZ led to a considerable shift in the ζ potentials to positive direction; ζ-potential shifted gradually from 12.5 ± 1.0 mV to 19.4 ± 0.9 mV, 34.0 ± 1.4

mV, and 36.4 ± 1.0 mV by heat treatment of LYZ solution for 1 hour, 3 hours, and 6 hours, respectively. This reflects that potential structural changes of LYZ caused by heating (at 90 °C) lead to a gradually enhanced exposure of positively charged moieties to the surface with increasing heating time up to 6 hours. Meanwhile, the mixture of PGM and LYZ showed a gradual shift of the $\zeta$ potential from neutral to negative direction. The very low $\zeta$ potential values ($|\zeta|$ less than 5 mV) of PGM/unheated and PGM/$1^{hr}$ heated LYZ mixtures thus support the aforementioned proposition that suppression of surface charges is mainly responsible for the enhanced adsorbed mass on nonpolar PDMS surface for PGM/LYZ mixtures compared to respective PGM or LYZ (section 3.2). On the other hand, the $\zeta$ potentials of PGM/$3^{hr}$ heated LYZ and PGM/$6^{hr}$ heated LYZ mixture were distinctively negative, even though the absolute values of positive $\zeta$ potentials of these heated LYZs are much larger than those of PGM. This is not straightforward to understand intuitively, and will be discussed in the Discussion section below.

### *3.4.Hydrodynamic diameter and size distribution: Dynamic light scattering (DLS)*

The interaction between PGM and LYZ as a function of the heating time of LYZ was further investigated by DLS. Figure 4 illustrates the changes in the intensity-weighted hydrodynamic size ($D_H$) distribution of PGM, un-/heat-treated LYZs, as well as their mixtures.

As is well known [28], the intensity-weighted display of DLS data has the advantage of showing particles with a broad range of sizes, including small ones, but larger particles tend to be exaggerated in the intensity. Thus, it should be noted that the intensity (%, in y-axis) is not scaled with the number population of particles. Two quantities are employed to present and compare the hydrodynamic sizes; firstly, the Z-averages of $D_H$ for the solutions are shown in Table 2. Z-average is a single value, representing an average for all the particles in the solution. Thus, despite its simplicity to compare, it could be misleading due to over-simplification, especially for bi- or multi-modal distribution of particles. Secondly, to focus on the main species present in the solution, $D_H$ size distribution of major peaks ($1^{st}$ only or $1^{st}$ and $2^{nd}$) was also analyzed and is presented in Figure 5.

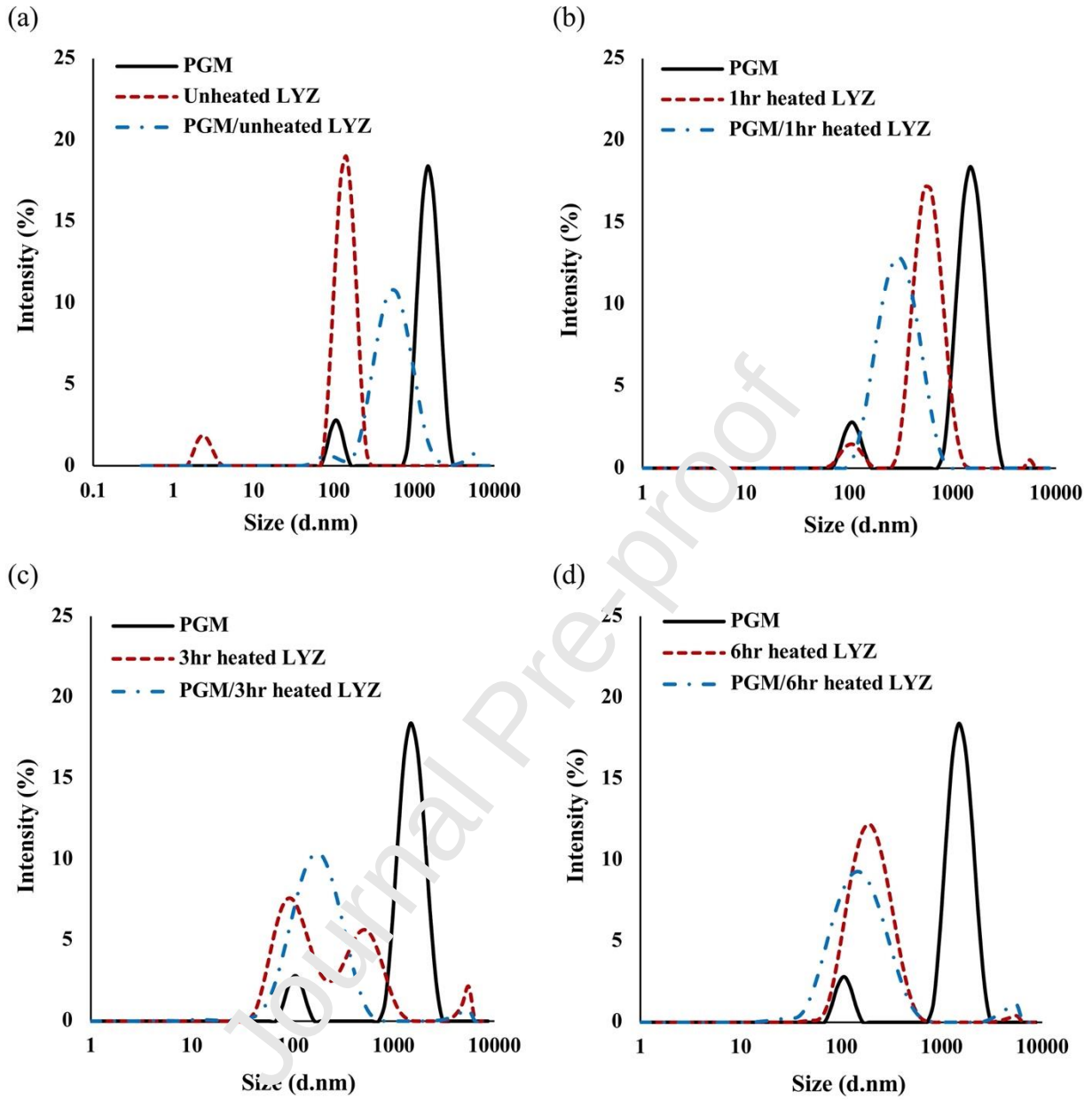


**Figure 4.** Intensity-weighted distribution of the hydrodynamic diameter $D_H$ for either individual or mixed components of (a) PGM/unheated LYZ, (b) PGM/$1^{hr}$ heated LYZ, (c) PGM/$3^{hr}$ heated LYZ and (d) PGM/$6^{hr}$ LYZ solutions. It is very likely that PGM physically "shrinks" upon interaction with all LYZ cases.

**Table 2.** Z-average of $D_H$ values obtained from DLS experiments.

| Solution | Z-average values (d.nm) | Solution | Z-average values (d.nm) |
|---|---|---|---|
| PGM | 1011.04 ± 65.5 | PGM/unheated LYZ | 443.48 ± 9.4 |

| | | | |
|---|---|---|---|
| Unheated LYZ | 174.26 ± 18.8 | PGM/1$^{hr}$ heated LYZ | 241.36 ± 6.5 |
| 1$^{hr}$ heated LYZ | 565.00 ± 42.4 | PGM/3$^{hr}$ heated LYZ | 148.06 ± 2.6 |
| 3$^{hr}$ heated LYZ | 169.4 ± 26.4 | PGM/6$^{hr}$ heated LYZ | 132.36 ± 1.0 |
| 6$^{hr}$ heated LYZ | 177.86 ± 1.3 | | |

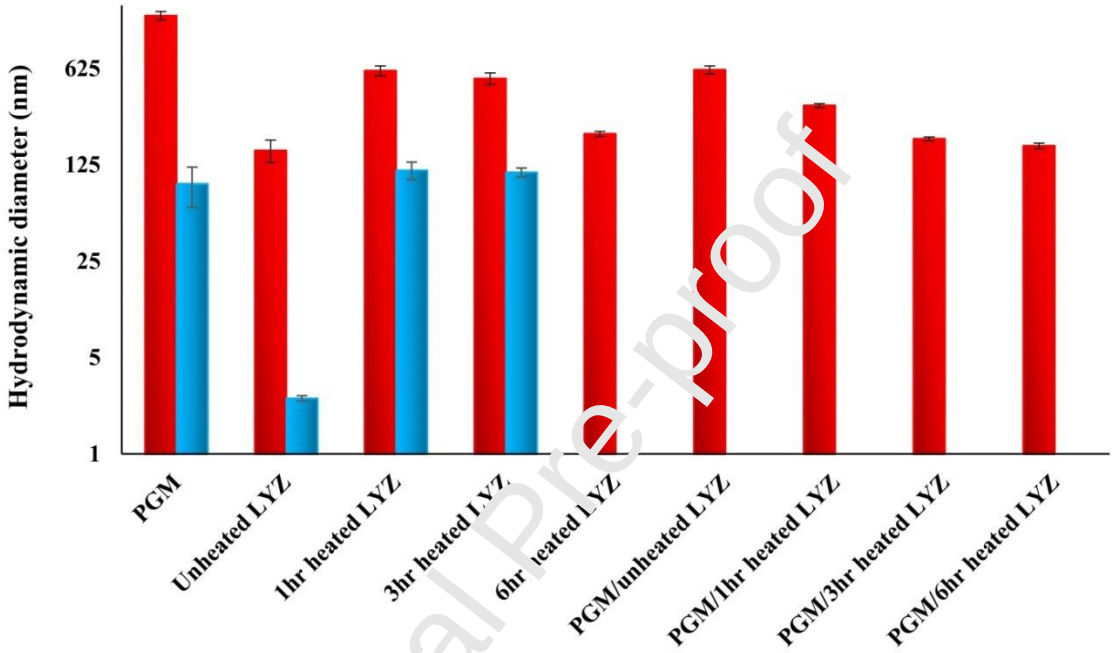


**Figure 5.** Major intensity-weighted distribution peaks of $D_H$ for PGM, un-/heat-treated LYZ and their mixtures solutions (red bars are the major intensity-weighted distribution peaks in the monodispersed size distributions or together with blue bars as the first and second major intensity-weighted distribution peaks in the bimodal size distributions).

All the solutions showed either bimodal/polydispersed (PGM, unheated LYZ, PGM/unheated LYZ, 1$^{hr}$ heated LYZ and 3$^{hr}$ heated LYZ) or monodispersed (the rest) size distributions. The polydispersity of PGM stems from its inherent self-aggregation and such behavior is consistent with previous studies [12-14]. Unheated LYZ displayed two populations at 2.6 ± 0.1 nm and 159.9 ± 29.3 nm; considering the molecular weight of LYZ (14.3 kg/mol), the peak at 2.6 nm may correspond to the monomer of LYZ whereas the peak at ca. 159.9 nm may correspond to its aggregates. It is well known that LYZ also has a high tendency to self-aggregate at high concentrations; heating of LYZ was reported to accelerate the aggregation due to conformational changes and intermolecular interaction in a previous study [19,20,29]. This

tendency is in line with the change of size distribution of between unheated LYZ and $1^{hr}$ heated LYZ in that the peak at 2.6 ± 0.1 nm disappeared and the main peak at 159.9 ± 29.3 nm (unheated) shifted to 604.6 ± 50.8 nm and 114.6 ± 16.9 nm as the first and second main peaks ($1^{hr}$ heated LYZ). However, extended heating of LYZ, e.g. up to 3 hours or 6 hours, resulted in rather a shrink in the overall size distribution compared to those of $1^{hr}$ heated LYZ; $3^{hr}$ heated LYZ showed the first and second main peaks at 530.4 nm ± 51.3 nm and 110.7 ± 8.5 nm, and $6^{hr}$ heated LYZ showed a single main peak at 210.42 ± 9.0 nm. Lastly, a large increase in $D_H$ after 1 hour heating of LYZ and subsequent reduction after extended heating for $3^{hr}$ or $6^{hr}$ heating, are observed from the Z-average values too (Table 2).

A comparison of the PGM/LYZ mixture solutions shows a gradual decrease in the $D_H$ distribution with increasing heating time of LYZ, namely PGM/unheated LYZ < PGM/$1^{hr}$ heated LYZ < PGM/$3^{hr}$ heated LYZ < PGM/$6^{hr}$ heated LYZ. This trend is consistent in the Z-average values too. However, it is more important to note how the $D_H$ distribution of each PGM/LYZ mixture is changed compared to those of respective PGM or LYZ before mixing. Here, PGM is by far the largest in $D_H$ and is fixed in size, as it was not heat-treated in this study. For PGM/unheated LYZ and PGM/$6^{hr}$ heated LYZ, the $D_H$ of the mixture is comparable to that of LYZ alone prior to mixing. In contrast, for PGM/$1^{hr}$ heated LYZ, the $D_H$ of the mixture is clearly smaller than $1^{hr}$ heated LYZ alone. This can be interpreted as that the associative interaction or complexation between PGM and LYZ is most effective for PGM/$1^{hr}$ heated LYZ mixture. The case of PGM/$3^{hr}$ heated LYZ is somewhat complex as the peak for PGM/$3^{hr}$ heated LYZ mixture lies between two main peaks of $3^{hr}$ heated LYZ (Figure 4 and 5). However, according to Table 2, the Z-average of PGM/$3^{hr}$ heated LYZ mixture is slightly smaller than that of $3^{hr}$ heated LYZ. Thus, it can be suggested that the associative interaction or complexation between PGM and $3^{hr}$ heated LYZ is not as strong as PGM/$1^{hr}$ heated LYZ, but stronger than the other pairs.

### *3.5.Conformational changes: CD spectroscopy*

Lastly, the conformational features of PGM, un-/heat-treated LYZ, and their mixture solutions were characterized by means of CD spectroscopy. Figure 6 displays the far-UV and the near-UV spectra of all solutions. The former and the latter are known to reflect the secondary and tertiary structures of the proteins, respectively.

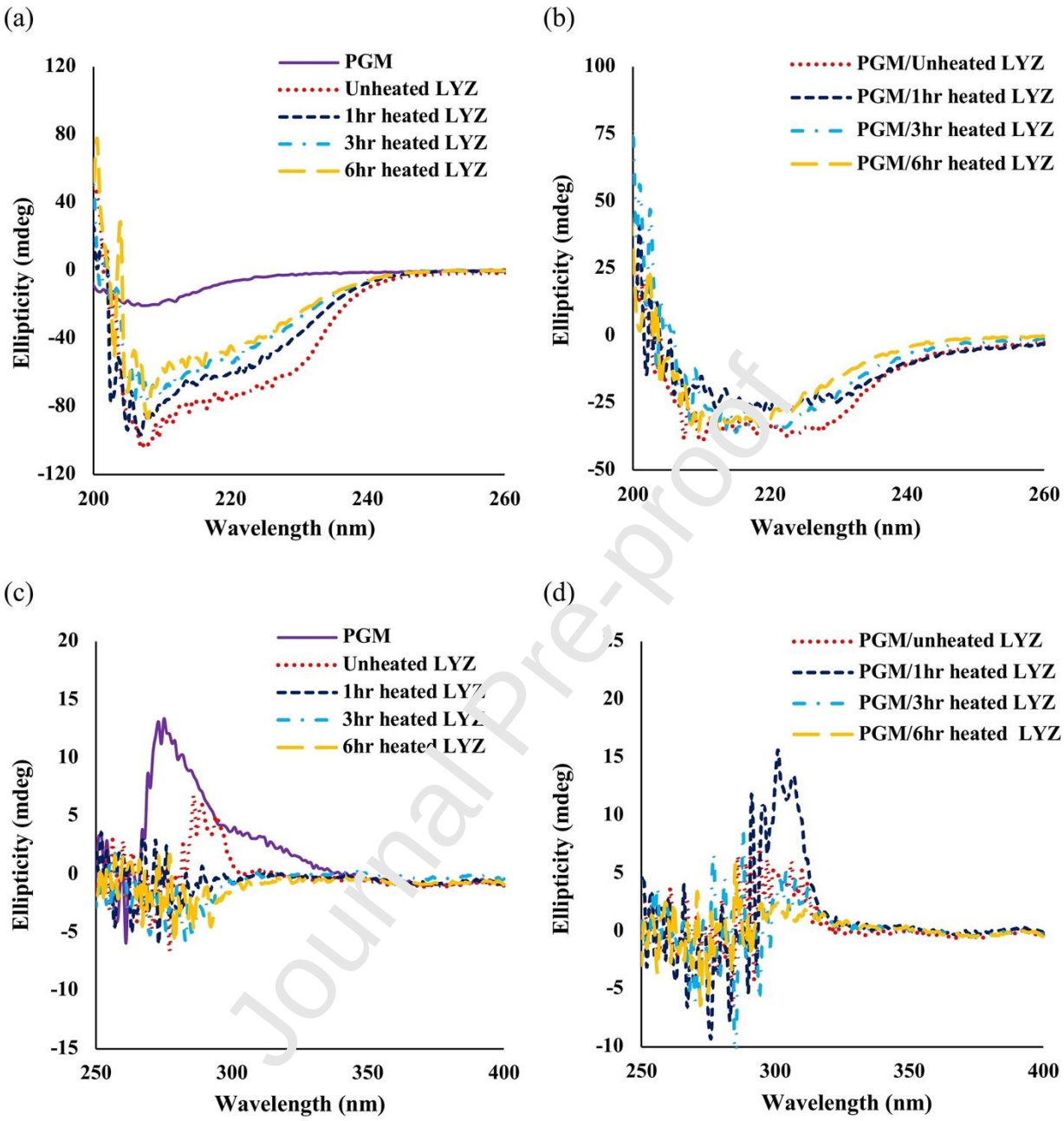


**Figure 6.** Changes in the secondary structure: Far-UV spectra of (a) PGM, unheated and heated LYZ and (b) the mixture of PGM and un-/heat-treated LYZ; Changes in the tertiary structure: Near-UV CD spectra of (c) PGM, unheated and heated LYZ and (d) the mixture of PGM and un-/heat-treated LYZ. The horizontal axes of far-UV CD graphs started at 200 nm due to very high noise in the spectra at lower wavelengths.

PGM showed a prominent negative peak centered at 206 nm in the far-UV CD spectrum, implying an overall random coil peptide structure [11]. Moreover, there was a prominent positive

peak at around 270 nm in the near-UV CD spectrum of PGM, which has been identified as a characteristic tertiary structural feature of PGM, originating from the hydrophobic moieties in the C- and N-terminal regions of PGM [11-14]. The presence of the peak in the wavelength range of 260-280 nm is generally associated with the aromatic side chains, existing in C- and N-terminal regions of mucins (hydrophobic parts of mucins) [30,31].

Far-UV spectra of unheated/heated LYZ solutions had negative bands in the range from 200 to 260 nm, which are characteristic of an α+β protein [32], with much higher intensities than PGM. The peaks at ~222 nm and ~208 nm reflect α-helix and the peak at ~216 nm denotes β–sheet structures, respectively [33]. According to previous studies, the native lysozyme in solution at pH~7 approximately consists of 36% a-helix, 15% *β*-sheet, 15% turn and 34% unordered secondary structure components [33,34]. It is most notable that the ellipticity of LYZ between 200 and 240 nm decreased with increasing heating time of LYZ. The decrease of the ellipticity between 208 and 230 nm may be attributed to a gradual loss of α-helix structures in LYZ with increasing heat treatment [34-36]. Near-UV CD spectra of unheated LYZ disclosed a weak, yet clear positive peak in the range of 280-310 nm. The exact position and intensity of this peak are different from those of PGM, but they are similar in that they represent characteristic tertiary structures of PGM and LYZ, respectively. The peaks at ~285, ~289 and ~293 nm are generally related to the contributions of tryptophan residues especially Trp 108 and Trp 62 [37,38]. Upon heating LYZ for 1 hour or longer, this peak disappeared and the near UV CD spectra became featureless, indicating the loss of the corresponding tertiary structure.

Upon mixing PGM with unheated or heated LYZ, the characteristic features of the secondary structure of LYZ in the far-UV CD spectra were significantly weakened in all PGM/LYZ mixtures. This could be due to the altered conformations of PGM and/or LYZ, following associative interaction between them, but also could be due to a simple dilution effect without any interaction. Individual CD spectra of PGM and LYZ are significantly different in the features and intensities, and the volume ratio (and weight ratio too) between PGM and LYZ in their mixture is 1:1. As a semi-quantitative means to evaluate a potential interaction between the two macromolecules, the experimentally acquired CD spectra of PGM/polycation mixture and the numerical average of two individual CD spectra namely, 0.5 × (the spectra of PGM + the spectra LYZ), were compared in previous studies [12-14]. The conjecture is that if the experimentally acquired spectra overlap with the numerical average, it is likely that the two

macromolecules are simply dispersed in the mixture solution without any interaction between them. This approach was applied to PGM/LYZ mixtures too and the results for far-UV CD spectra are shown in the Supplementary information (Figure S1).

In all cases, the experimentally determined far-UV CD spectra of the mixture and the numerical average of individual spectra of PGM and LYZ were clearly different, suggesting that associative interaction do occur between PGM and LYZ. Furthermore, in all cases, the peak intensity of the experimentally determined spectra of PGM/LYZ mixtures was smaller than that of the numerical average. It is also notable that the extent of deviation from each other was most significant for PGM/$1^{hr}$ heated LYZ, followed by PGM/$3^{hr}$ heated LYZ, and the others.

The analysis according to the comparison between the experimentally determined spectra of PGM/LYZ mixtures and the numerical averages of the two respective spectra was applied to near-UV CD spectra as well, and the results are shown in Figure S2.

Basically, the same trend with far-UV CD spectra was observed in that the two spectra were not overlapped with each other for all cases. Nevertheless, the comparison of the near-UV CD spectra before and after mixing PGM and LYZ, as shown in Figure 6(c) and (d), already shows a couple of outstanding differences too. Firstly, the distinctive peak for PGM at ca. 270 nm has completely disappeared after mixing with LYZ in all cases. It is interesting to note that this was observed from PGM/polycation pairs in previous studies too [12-14], but only from those displaying an effective synergistic lubrication. In this study, however, this feature was observed from all cases. Secondly, a strong positive peak centered at around 308 nm appeared after mixing PGM and LYZ, but only for PGM/$1^{hr}$ heated LYZ mixture. It should be stressed that this peak is not an intermediate between the characteristic peaks of PGM and unheated LYZ, in terms of both peak position and intensity, but completely new. Meanwhile, all the other PGM/LYZ mixtures showed no signals in the near-UV CD spectra.

## 4. Discussion

The key question of this study was whether lysozyme (LYZ) may function as an artificial crosslinker for PGM to present synergistic lubricating properties at PDMS/PDMS interface, similar to some synthetic polycations in previous studies [12-14]. Even though only a few polycations have been studied to date, there are a couple of common behaviors of PGM/polycation mixture systems that are successful in displaying an effective synergistic

lubrication. (1) A complexation between PGM and polycations leads to charge neutrality; since the sliding surface was nonpolar PDMS in those studies, suppression of charges enhances the adsorption of the PGM/polycation aggregates as well as the lubricity. (2) A significant contraction in the hydrodynamic size of PGM/polycations occurs in the course of complexation between PGM and polycation; as the PGM/polycations are not covalently bonded to PDMS surface, but continuously detached and re-adsorbed at the surface during tribological contacts, smaller size is beneficial for easy convection and reformation of PGM/polycations aggregates as lubricating films [12-14]. Moreover, the extent of contraction reflects the efficacy of electrostatic attraction between PGM and polycation as well.

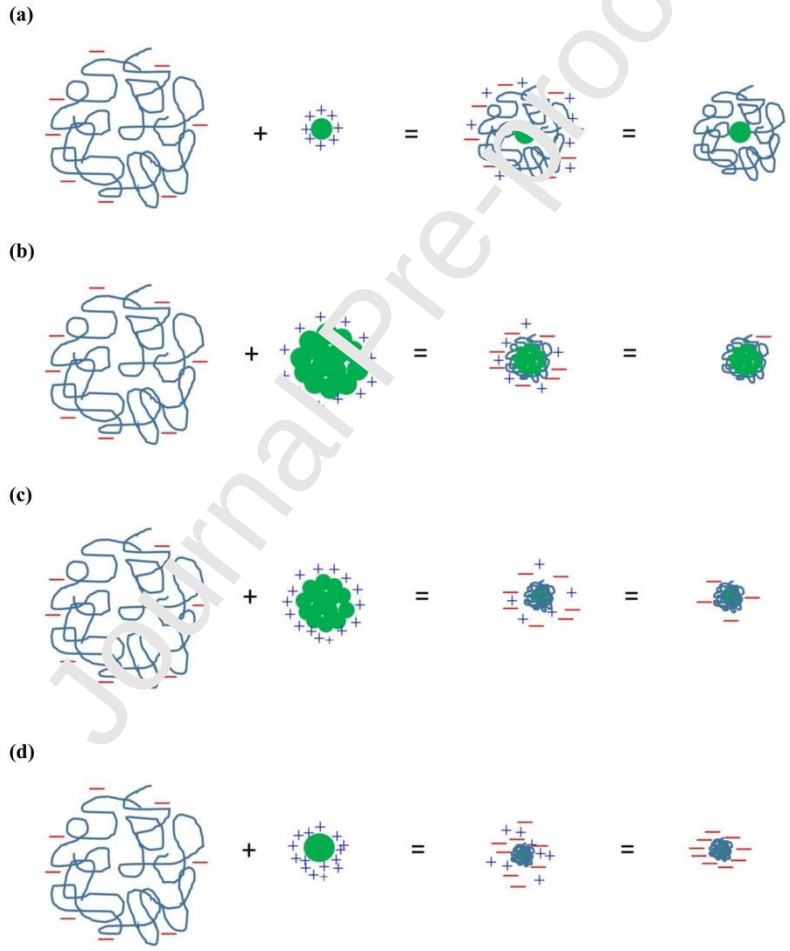


**Figure 7.** A schematic illustration of the interaction between PGM and lysozyme as (a) PGM/unheated LYZ: the size of the mixture is an intermediate between PGM and LYZ, the charge is neutral; (b) PGM/$1^{hr}$ heated LYZ: a shrink occurs, the mixture is nearly neutral; (c) PGM/$3^{hr}$ heated LYZ: a moderate shrink occurs, the mixture is quite charged; (d) PGM/$6^{hr}$ heated LYZ: a moderate shrink is observed, and the mixture is highly charged.

Given that LYZ is a polycation (IEP ~ 11) with the molecular weight (14.3 kDa) comparable to b-PEI or l-PEI in the previous studies, a synergistic lubricating effect is readily expected from PGM/LYZ pairs too. However, unlike synthetic polycations, which are mostly random-coil in their conformation, LYZ has a very well-defined protein structure that may play as an additional factor affecting the interaction with PGM. Modulation of the protein structure of LYZ by heat treatment in this study thus provides an opportunity to investigate the role of the structure of artificial crosslinker in the complexation with PGM and consequent synergistic lubrication.

To establish a holistic understanding of the structural changes of LYZ and PGM/LYZ complex as a function of heating time of LYZ, a schematic illustration combining the data on hydrodynamic size ($D_H$), conformational structure and zeta potential for each pair of PGM/LYZ is presented in Figure 7.

The first important point to note in Figure 7 is that the hydrodynamic size of unheated LYZ, illustrated by a green circle, does not represent the size of an individual LYZ molecule, but of an aggregate of LYZ. As briefly mentioned above, LYZ has a strong tendency for self-aggregation, driven by hydrophobic interactions between them. In turn, this is based on the amphiphilic nature of LYZ. The lubricating capabilities of LYZ alone (Figure 1) are surprisingly good in high-speed regime (≥ 10 mm/s) and even superior to PGM. An excellent lubricity at high-speed regime, but a poor lubricity at low-speed regime is a typical behavior observed from small, amphiphilic macromolecules such as a polyethylene-polypropylene-polyethylene (PEO-PPO-PEO) triblock copolymer "F68" [39] or a type of hydrophobin, "HBFI" [39]. A substantial increase in $D_H$ upon heating LYZ was also previously reported [19,20,29]. A new finding from the present study is that while the $D_H$ of LYZ initially increased from heating (e.g. 1 hour at 90 °C), an extended heating, such as for 3 hours or 6 hours, rather reduced the $D_H$ compared to $1^{hr}$ heated LYZ aggregates. This could be possibly because an extended heat energy to the heated LYZ solution starts to split the aggregates into smaller ones.

Secondly, the zeta potential of LYZ is gradually shifting towards the positive direction with increasing heating time. This can be explained by the strengthened hydrophobic interaction at the core of the LYZ aggregates with increasing heat energy and increasing placement of positively charged moieties on the surface [40,41]. However, mixing of PGM with LYZ resulted in a shift of zeta potential from a neutral to the negative direction with increasing heating time of LYZ,

even though the absolute zeta potential values of heated LYZ, $|\zeta|$, are clearly larger than that of PGM (Figure 3). This is difficult to understand if we consider the electrostatic charge aspect only. One possible explanation for this behavior is that the aggregates of heated LYZ are disintegrated into smaller ones in the course of interaction with PGM. Since the driving force of self-aggregation between LYZs is hydrophobic interaction, electrostatic attraction with PGM may overwhelm the weaker hydrophobic interaction, leading to a complexation between PGM with smaller aggregates of LYZ, and overall negative zeta potentials of the PGM/LYZ aggregates. Of course, this is limited to the pairs of PGM/$3^{hr}$ heated LYZ and PGM/$6^{hr}$ heated LYZ, and the net negative charges on these aggregates can oppose the effective synergistic lubrication. Moreover, the inferior lubricity of PGM/$6^{hr}$ heated LYZ of the two (Figure 1) is in line with a greater negative charge of this pair (Figure 3).

Meanwhile, the lack of synergistic lubrication by PGM/unheated LYZ pair, despite an excellent charge neutralization and a facilitated surface adsorption, can be associated with a weak contraction in $D_H$, in turn, a less intimate interaction between PGM and unheated LYZ. In fact, PGM/unheated LYZ is the only pair that showed an intermediate $D_H$ between those of PGM and LYZ, respectively, whereas all the other pairs displayed even smaller $D_H$ of PGM/LYZ mixtures than that of LYZ alone. In other words, even though PGM and unheated LYZ do interact via electrostatic attraction, the well-defined secondary and tertiary structure of LYZ may act as a barrier for a stronger attraction between PGM and LYZ required for synergistic lubrication. In this regard, CD spectroscopy studies have clearly demonstrated that unheated LYZ has a most distinct structure in both far-UV and near-UV CD spectra (Figure 6). Unheated LYZ (or native lysozyme) is known as a "rigid" protein and often resists significant conformational changes in contact with several surfaces possessing different groups [42-44]. Moreover, the comparison between the experimentally acquired CD spectra of PGM/LYZ and the numerical average between PGM and LYZ has revealed that PGM/$1^{hr}$ heated LYZ pair is the one that deviates from each other most significantly in both far-UV CD (Figure S1) and near-UV CD spectra (Figure S2). In turn, this means that the extent of structural alteration of PGM and/or LYZ caused by the interaction with each other is the highest for PGM/$1^{hr}$ heated LYZ pair. Here, it is important to emphasize that this is not because LYZ has undergone the most significant structural changes after heating for 1 hour than other heating conditions. As shown in Figure 6, the secondary structural features of LYZ were increasingly weakened upon heating up to 6

hours, and the tertiary structural feature of LYZ was lost for all heated LYZ samples. Thus, a more plausible scenario is that LYZ reached an optimum conformation to interact with PGM in a most intimate and effective manner after heating for 1 hour. Additional heating of LYZ than 1 hour might have compromised this optimum conformation due to further structural changes.

Lastly, how an intimate complexation between PGM and $1^{hr}$ heated LYZ, as well as some synthetic polycations in previous studies, leads to a synergistic and very effective lubricity at PDMS/PDMS interface is not a question that can be answered based on direct experimental data yet. Nevertheless, it can be deduced from general conditions that are necessary for amphiphilic (co)polymers to act as an effective lubricant additive at a hydrophobic interface in an aqueous environment [45-47]. For amphiphilic (co)polymers, regardless of the detailed structure or origin, hydrophobic parts function as anchoring groups onto the hydrophobic or nonpolar surface, and hydrophilic parts attract water to form an aqueous lubricating film. Thus, less ordered structure of hydrophobic parts would be more beneficial to adsorb onto hydrophobic tribo-surfaces as less energy to rearrange the conformation is necessary for this course. This is critically important during tribological contact in pin-on-disk tribometry, because, as addressed above, the cycle of initial adsorption > tribostress-induced desorption > re-adsorption is continuously taking place in a short time scale. In this regard, if the structure of proteins, especially tertiary structure originating from hydrophobic moieties, were sustained, it could become a factor to retard the adsorption of proteins with the nonpolar tribo-surface because a rearrangement of the hydrophobic part is required for surface adsorption. Thus, the presentation of respective characteristic peaks for both PGM and LYZ in near-UV CD spectra prior to mixing with each other (Figure 6(c)) is one of the major factors responsible for their poor lubricity. In the same context, the disappearance of both peaks in the PGM/1hr heated LYZ aggregates is also associated with the excellent lubricity after mixing (Figure 6(d)). Unlike the case of PGM/polycations in the previous studies though [12-14], the occurrence of a new peak in near-UV CD spectra for PGM/$1^{hr}$ heated LYZ (Figure 6(d)) is a unique feature of this protein-protein complexation. While further detailed conformational characteristics of PGM/LYZ cannot be unraveled by CD spectroscopy and other analytical tools in this study, especially at the water/PDMS interface, we propose that this emerging feature has very little to do with adsorption of the aggregate onto PDMS surface.

As mentioned earlier, mucins are part of mucous membranes covering the epithelial tissue surfaces in the respiratory tract, the gastrointestinal tract, the reproductive system, and the ocular surface in order to lubricate and protect them [1]. On the other hand, lysozyme is an antimicrobial protein that has antiviral, anti-inflammatory, antioxidant, and anti-nociceptive properties in both native and heat-treated forms [48]. Lysozyme is also found in saliva, tears, blood serum, the gastrointestinal tract, the respiratory tract, and the genitourinary system [49]. Taking into account the most likely interaction of mucin and lysozyme in the biological environment [50], such findings of this research not only can shed light on the physicochemical mechanisms behind the complexation between mucinous glycoproteins and lysozyme with an emphasis on the synergistic lubricating properties but also can contribute towards food and biopharmaceutical industries.

## 5. Conclusions

In this study, the possibility of lysozyme (LYZ) functioning as an artificial crosslinker for PGM to display enhanced and synergistic aqueous lubricating properties based on its distinctive positive charge characteristics in a neutral aqueous environment and electrostatic complexation with PGM was explored. Compared to synthetic polycations that showed an excellent synergistic lubricity with PGM in previous studies, for instance, b-PEI and chitosan, LYZ has two unique structural features. Firstly, LYZ has its own secondary and tertiary protein structures, which impart some degree of rigidity, and are subject to change by heat treatment. Secondly, due to its amphiphilicity, LYZ is present as an aggregate via self-assembly, which is also subject to change by heat treatment in the charge characteristics and size distribution. Thus, this study has provided an opportunity to study the role of the structure of polycationic crosslinker in association with PGM and synergistic lubrication. In a variation of heating time from 0, 1, 3, and 6 hours at 90 °C, LYZ has shown a gradual loss of its characteristic secondary structure, whereas heating LYZ for 1 hour has already removed the characteristic tertiary structure according to CD spectroscopy studies. Meanwhile, the electrostatic neutrality was achieved only for PGM/unheated LYZ and PGM/$1^{hr}$ heated LYZ pairs, PGM/$3^{hr}$ heated LYZ and PGM/$6^{hr}$ heated LYZ pairs showed net negative zeta potentials. Among many LYZ samples with varying duration of heat treatment to interact with PGM, PGM/$1^{hr}$ heated LYZ is the only pair in this study that meets both conditions to display synergistic lubrication in previous studies, namely electrostatic neutrality and a

significant contraction upon complexation, and of course the most effective lubrication properties. In turn, this study dictates that electrostatic attraction is not a sufficient condition to select or design polycationic macromolecules as an artificial crosslinker to compensate weak aggregation properties of commercially available PGM and to enhance its lubricating properties.

**References**


[1] Taherali F, Varum F, Basit AW. A slippery slope: On the origin, role and physiology of mucus. Advanced drug delivery reviews. 2018 Jan 15;124:16-33.

[2] Bansil R, Turner BS. The biology of mucus: Composition, synthesis and organization. Advanced drug delivery reviews. 2018 Jan 15;124:3-15.

[3] Strous GJ, Dekker J. Mucin-type glycoproteins. Critical reviews in biochemistry and molecular biology. 1992 Jan 1;27(1-2):57-92.

[4] Pakkanen KI, Madsen JB, Lee S. Conformation of bovine submaxillary mucin layers on hydrophobic surface as studied by biomolecular probes. International journal of biological macromolecules. 2015 Jan 1;72:790-6.

[5] Rickert CA, Wittmann B, Fromme R, Lieleg O. Highly transparent covalent mucin coatings improve the wettability and tribology of hydrophobic contact lenses. ACS Applied Materials & Interfaces. 2020 May 28;12(25):28074-83.

[6] Rickert CA, Lutz TM, Marczynski M, Lieleg O. Several Sterilization Strategies Maintain the Functionality of Mucin Glycoproteins. Macromolecular Bioscience. 2020 Jul;20(7):2000090.

[7] Marczynski M, Winkeljann B, Lieleg O. Advances in Mucin Biopolymer Research: Purification, Characterization, and Applications. Biopolymers for Biomedical and Biotechnological Applications. 2021 Feb 23:181-208

[8] Lee S, Biresaw G, Mittal KL. Aqueous Lubrication with Polyelectrolytes: Toward Engineering Applications. inSurfactants in Tribology 2017 Sep 11 (pp. 39-60). CRC Press.

[9] Madsen JB, Sotres J, Pakkanen KI, Efler P, Svensson B, Abou Hachem M, Arnebrant T, Lee S. Structural and mechanical properties of thin films of bovine submaxillary mucin versus porcine gastric mucin on a hydrophobic surface in aqueous solutions. Langmuir. 2016 Sep 27;32(38):9687-96.

[10] Schömig VJ, Käsdorf BT, Scholz C, Bidmon K, Lieleg O, Berensmeier S. An optimized purification process for porcine gastric mucin with preservation of its native functional properties. RSC advances. 2016;6(50):44932-43.

[11] Lee S, Müller M, Rezwan K, Spencer ND. Porcine gastric mucin (PGM) at the water/poly (dimethylsiloxane)(PDMS) interface: influence of pH and ionic strength on its conformation, adsorption, and aqueous lubrication properties. Langmuir. 2005 Aug 30;21(18):8344-53.

[12] Nikogeorgos N, Patil NJ, Zappone B, Lee S. Interaction of porcine gastric mucin with various polycations and its influence on the boundary lubrication properties. Polymer. 2016 Sep 25;100:158-68.

[13] Patil NJ, Rishikesan S, Nikogeorgos N, Guzzi R, Lee S, Zappone B. Complexation and synergistic boundary lubrication of porcine gastric mucin and branched poly (ethyleneimine) in neutral aqueous solution. Soft matter. 2017;13(3):590-9.

[14] Nikogeorgos N, Efler P, Kayitmazer AB, Lee S. "Bio-glues" to enhance slipperiness of mucins: improved lubricity and wear resistance of porcine gastric mucin (PGM) layers assisted by mucoadhesion with chitosan. Soft Matter. 2015;11(3):489-98.

[15] Benkerroum N. Antimicrobial activity of lysozyme with special relevance to milk. African Journal of Biotechnology. 2008;7(25).

[16] Abeyrathne ED, Lee HY, Ahn DU. Egg white proteins and their potential use in food processing or as nutraceutical and pharmaceutical agents—A review. Poultry science. 2013 Dec 1;92(12):3292-9.

[17] Cozzone PJ, Opella SJ, Jardetzky O. The effect of temperature on the structure of lysozyme in solution. InEnvironmental Effects on Molecular Structure and Properties 1976 (pp. 517-527). Springer, Dordrecht.

[18] Ibrahim HR. On the novel catalytically-independent antimicrobial function of hen egg-white lysozyme: A conformation-dependent activity. Food/Nahrung. 1998 Aug;42(03-04):187-93.

[19] Lewis EN, Qi W, Kidder LH, Amin S, Kenyon SM, Blake S. Combined dynamic light scattering and Raman spectroscopy approach for characterizing the aggregation of therapeutic proteins. Molecules. 2014 Dec;19(12):20888-905.

[20] Islam S, Shahzadi Z, Mukhopadhyay C. Temperature dependent aggregation mechanism and pathway of lysozyme: By all atom and coarse grained molecular dynamics simulation. Journal of Molecular Graphics and Modelling. 2021 Mar 1;103:107816.

[21] De Feijter J, Benjamins DJ, Veer FA. Ellipsometry as a tool to study the adsorption behavior of synthetic and biopolymers at the air–water interface. Biopolymers: Original Research on Biomolecules. 1978 Jul;17(7):1759-72.

[22] Vörös J, Ramsden JJ, Csucs G, Szendrő I, De Paul SM, Textor M, Spencer ND. Optical grating coupler biosensors. Biomaterials. 2002 Sep 1;23(17):3699-710.

[23] Marczynski M, Baier BN, Jiang K, Lutz TM, Crouzier T, Lieleg O. Charged glycan residues critically contribute to the adsorption and lubricity of mucins. Colloids and Surfaces B: Biointerfaces. 2020 Mar 1;187:110614.

[24] Çelebioğlu HY, Lee S, Chronakis IS. Interactions of salivary mucins and saliva with food proteins: A review. Critical reviews in food science and nutrition. 2020 Jan 2;60(1):64-83.

[25] Tangpasuthadol V, Pongchaisirikul N, Hoven VP. Surface modification of chitosan films: Effects of hydrophobicity on protein adsorption. Carbohydrate Research. 2003 Apr 22;338(9):937-42.

[26] Sarmiento F, Ruso JM, Prieto G, Mosquera V. ζ-Potential Study on the Interactions between Lysozyme and Sodium n-Alkylsulfates. Langmuir. 1998 Sep 29;14(20):5725-9.

[27] Pan X, Yu S, Yao P, Shao Z. Self-assembly of β-casein and lysozyme. Journal of colloid and interface science. 2007 Dec 15;316(2):405-12.

[28] Falke S, Betzel C. Dynamic Light Scattering (DLS). InRadiation in Bioanalysis 2019 (pp. 173-193). Springer, Cham.

[29] Kudou M, Shiraki K, Fujiwara S, Imanaka T, Takagi M. Prevention of thermal inactivation and aggregation of lysozyme by polyamines. European Journal of Biochemistry. 2003 Nov;270(22):4547-54.

[30] Kelly SM, Price NC. The use of circular dichroism in the investigation of protein structure and function. Current protein and peptide science. 2000 Dec 1;1(4):349-84.

[31] Kelly SM, Jess TJ, Price NC. How to study proteins by circular dichroism. Biochimica et Biophysica Acta (BBA)-Proteins and Proteomics. 2005 Aug 10;1751(2):119-39.

[32] Fasman GD, editor. Circular dichroism and the conformational analysis of biomolecules. Springer Science & Business Media; 2013 Nov 11.

[33] Greenfield NJ, Fasman GD. Computed circular dichroism spectra for the evaluation of protein conformation. Biochemistry. 1969 Oct;8(10):4108-16.

[34] Day L, Zhai J, Xu M, Jones NC, Hoffmann SV, Webster TJ. Conformational changes of globular proteins adsorbed at oil-in-water emulsion interfaces examined by Synchrotron Radiation Circular Dichroism. Food Hydrocolloids. 2014 Jan 1;34:78-87.

[35] Wu FG, Luo JJ, Yu ZW. Unfolding and refolding details of lysozyme in the presence of β-casein micelles. Physical Chemistry Chemical Physics. 2011;13(8):3429-36.

[36] Miller DP, Bell JK, McDowell JV, Conrad DH, Burgner JW, Héroux A, Marconi RT. Structure of factor H binding protein B (FhbB) of the periopathogen, Treponema denticola: insights into the progression of periodontal disease. Journal of Biological Chemistry. 2012 Feb 24:jbc-M112.

[37] Ikeda K, HAMAGUGHI K. The Binding of N-Acetylglucosamine to Lysozyme. The Journal of Biochemistry. 1969 Oct 25;66(4):513-20.

[38] Ikeda K, HAMAGUCHI K. A Tryptophyl Circular Dichroic Band at 305mμ of Hen Egg-white Lysozyme. The Journal of Biochemistry. 1972 Feb 25;71(2):265-73.

[39] Lee S, Røn T, Pakkanen H, Linder M. Hydrophobins as aqueous lubricant additive for a soft sliding contact. Colloids and Surfaces B: Biointerfaces. 2015 Jan 1;125:264-9.

[40] Carlsson F, Malmsten M, Linse P. Monte Carlo simulations of lysozyme self-association in aqueous solution. The Journal of Physical Chemistry B. 2001 Dec 6;105(48):12189-95.

[41] Kundu S, Aswal VK, Kohlbrecher J. Synergistic effect of temperature, protein and salt concentration on structures and interactions among lysozyme proteins. Chemical Physics Letters. 2016 Jul 16;657:90-4.

[42] Fröberg JC, Arnebrant T, McGuire J, Claesson PM. Effect of structural stability on the characteristics of adsorbed layers of T4 lysozyme. Langmuir. 1998 Jan 20;14(2):456-62.

[43] Norde W. The behavior of proteins at interfaces, with special attention to the role of the structure stability of the protein molecule. InBiologically Modified Polymeric Biomaterial Surfaces 1992 (pp. 85-91). Springer, Dordrecht.

[44] Wertz CF, Santore MM. Adsorption and reorientation kinetics of lysozyme on hydrophobic surfaces. Langmuir. 2002 Feb 19;18(4):1190-9.

[45] Røn T, Javakhishvili I, Jeong S, Jankova K, Lee S. Low friction thermoplastic polyurethane coatings imparted by surface segregation of amphiphilic block copolymers. Colloid and Interface Science Communications. 2021 Sep 1;44:100477.

[46] Lee S, Røn T, Pakkanen KI, Linder M. Hydrophobins as aqueous lubricant additive for a soft sliding contact. Colloids and Surfaces B: Biointerfaces. 2015 Jan 1;125:264-9.

[47] Røn T, Javakhishvili I, Jankova K, Hvilsted S, Lee S. Adsorption and aqueous lubricating properties of charged and neutral amphiphilic diblock copolymers at a compliant, hydrophobic interface. Langmuir. 2013 Jun 25;29(25):7782-92.

[48] Carrillo W, Spindola H, Ramos M, Recio I, Carvalho JE. Anti-inflammatory and anti-nociceptive activities of native and modified hen egg white lysozyme. Journal of medicinal food. 2016 Oct 1;19(10):978-82.

[49] Hankiewicz J, Swierczek E. Lysozyme in human body fluids. Clinica chimica acta. 1974 Dec 17;57(3):205-9.

[50] Filatova L, Emelianov G, Balabushevich N, Klyachko N. Supramolecular assemblies of mucin and lysozyme: formation and physicochemical characterization. Process Biochemistry. 2021 Dec 20;113:97-106.

**Highlights**

Biological lubricants play a vital role to minimize wear and dissipation of energy in living organisms and bio-devices.

Both porcine gastric mucin (PGM) and lysozyme (LYZ) solutions has poor lubricating properties in the boundary lubrication regime.

Lysozyme (LYZ), due to its distinctive positive charge characteristics in neutral aqueous environment, is expected to function as artificial crosslinker for PGM and display the synergistic aqueous lubricating properties.

Among four LYZ groups with different duration of heat treatment to interact with PGM, only PGM/1$^{hr}$ heated LYZ solution exhibits an excellent lubricity.

Excellent lubricity of PGM/1$^{hr}$ heated LYZ may come from surface charge compensation, tenaciously compact aggregation, unique conformational structure and considerable mass adsorption onto PDMS.

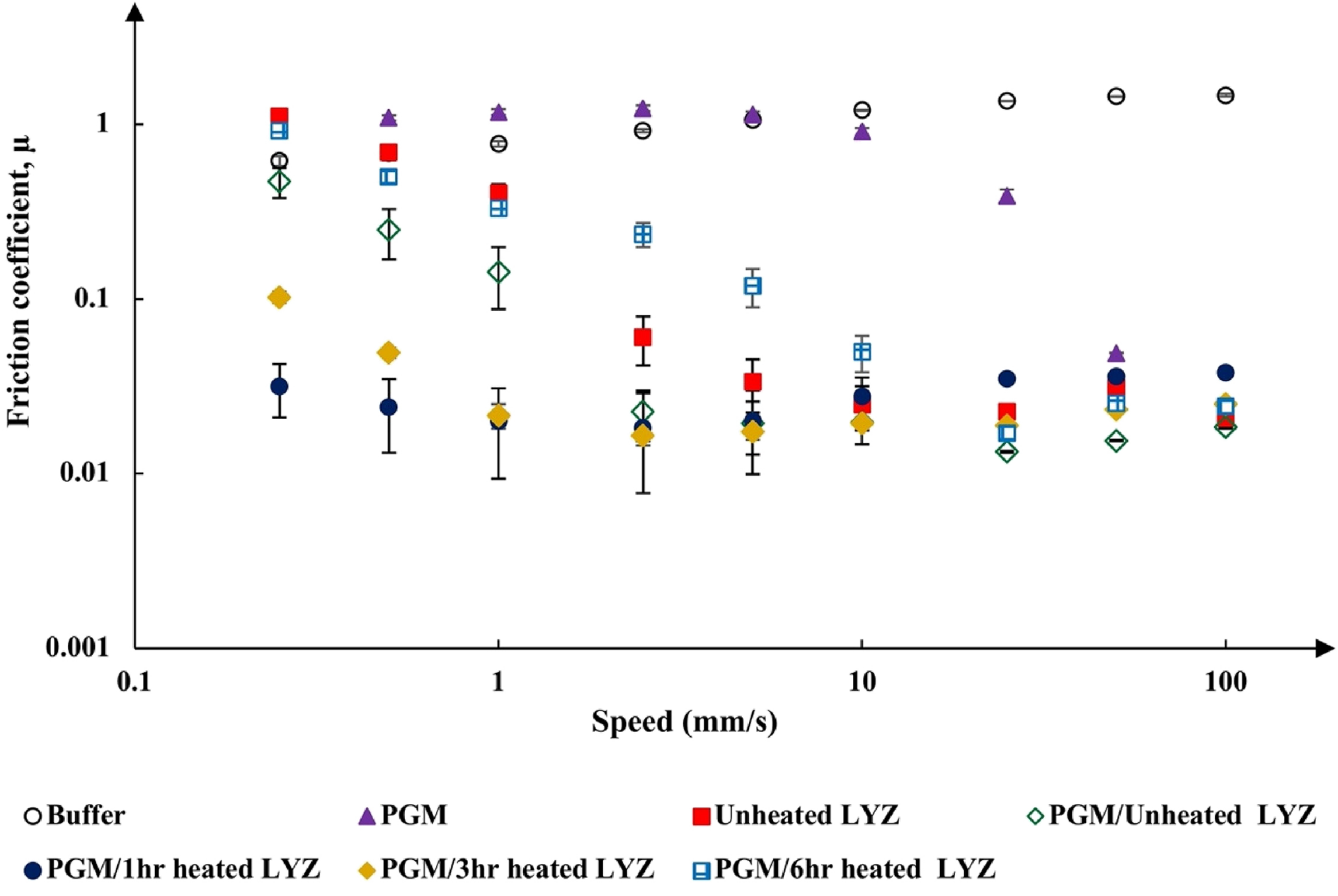
Friction coefficient, μ
1
0.1
0.01
0.001
0.1
1
10
100
Speed (mm/s)
Buffer
PGM
Unheated LYZ
PGM/Unheated LYZ
PGM/1hr heated LYZ
PGM/3hr heated LYZ
PGM/6hr heated LYZ

Figure 1

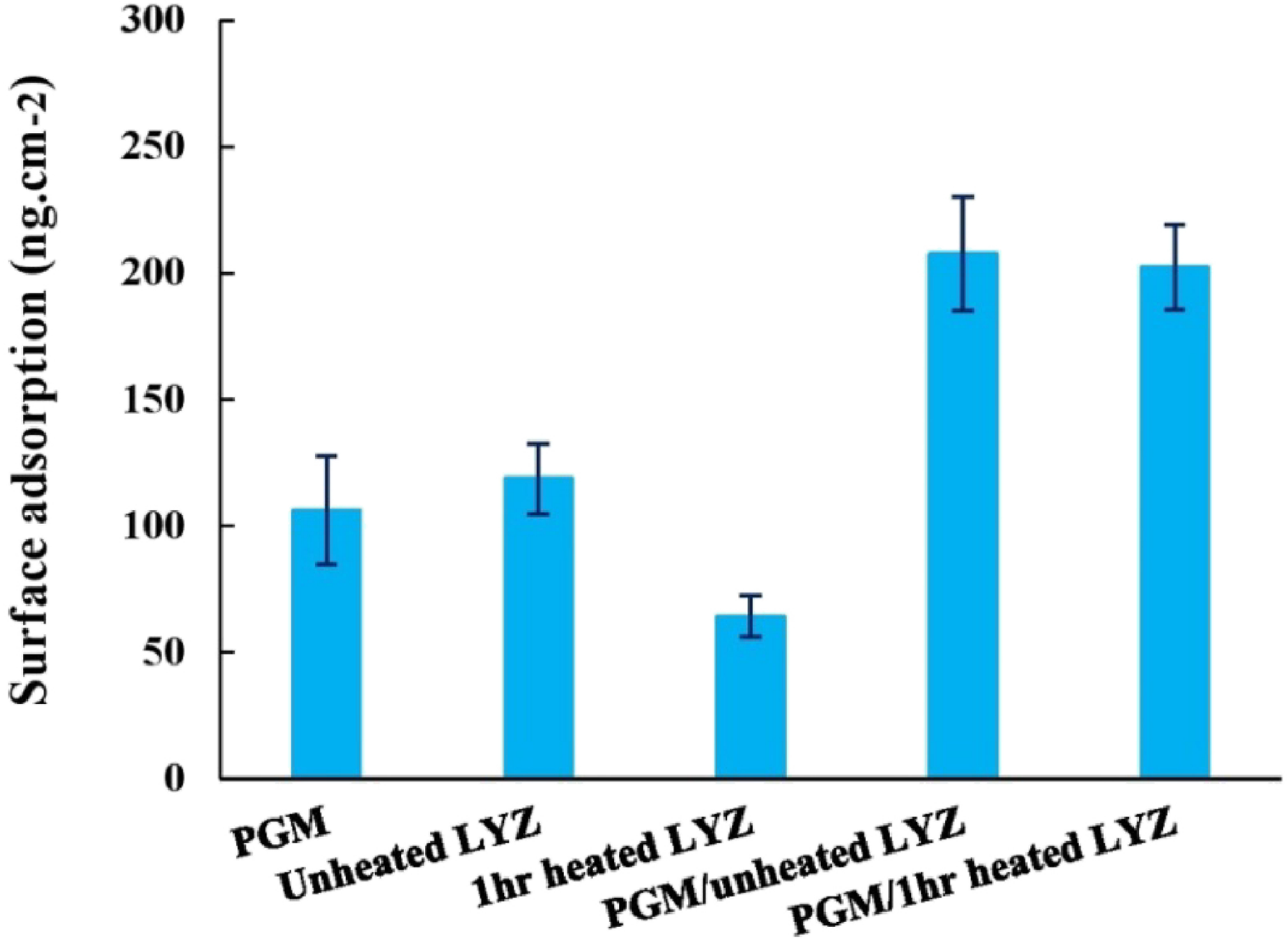
Surface adsorption (ng.cm-2)
300
250
200
150
100
50
0
PGM
Unheated LYZ
1hr heated LYZ
PGM/unheated LYZ
PGM/1hr heated LYZ

Figure 2

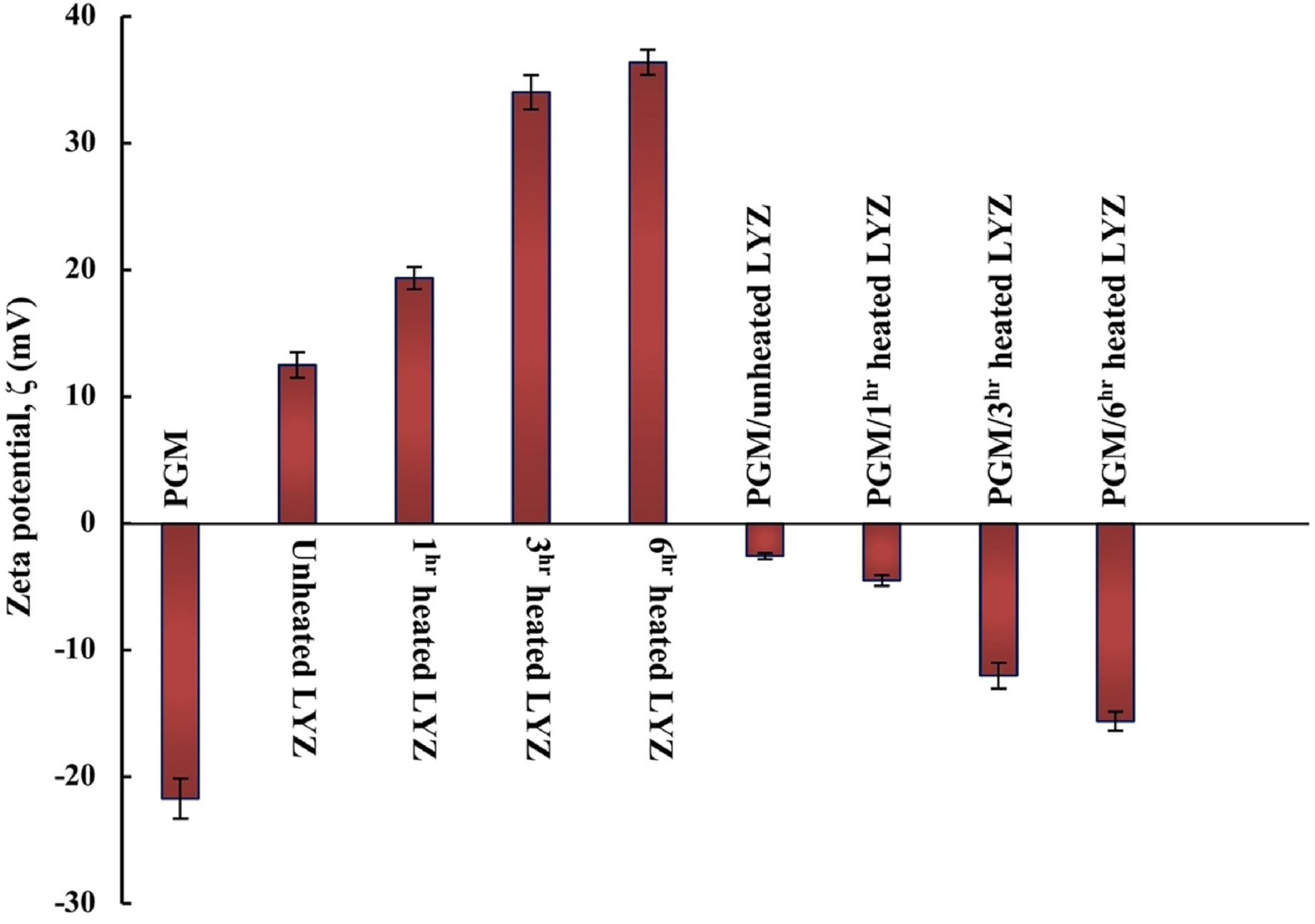
Zeta potential, ζ (mV)
40
30
20
10
0
-10
-20
-30
PGM
Unheated LYZ
1hr heated LYZ
3hr heated LYZ
6hr heated LYZ
PGM/unheated LYZ
PGM/1hr heated LYZ
PGM/3hr heated LYZ
PGM/6hr heated LYZ

Figure 3

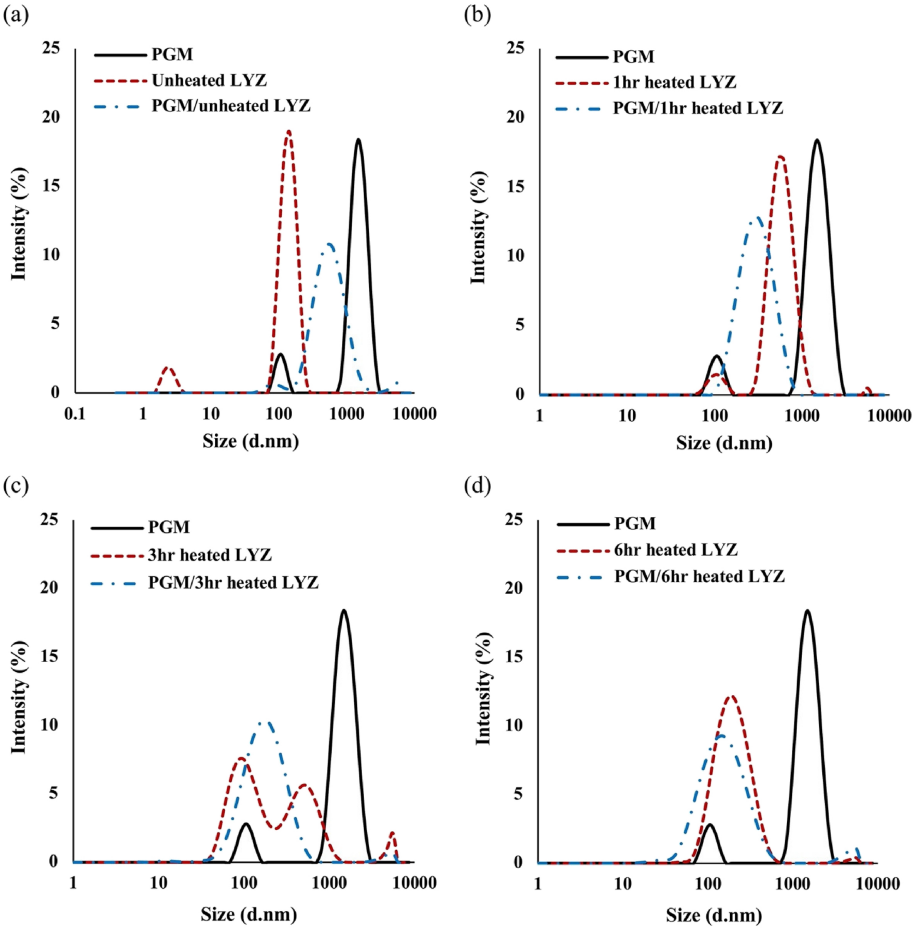
(a)
PGM
Unheated LYZ
PGM/unheated LYZ
Intensity (%)
Size (d.nm)
(b)
PGM
1hr heated LYZ
PGM/1hr heated LYZ
Intensity (%)
Size (d.nm)
(c)
PGM
3hr heated LYZ
PGM/3hr heated LYZ
Intensity (%)
Size (d.nm)
(d)
PGM
6hr heated LYZ
PGM/6hr heated LYZ
Intensity (%)
Size (d.nm)

Figure 4

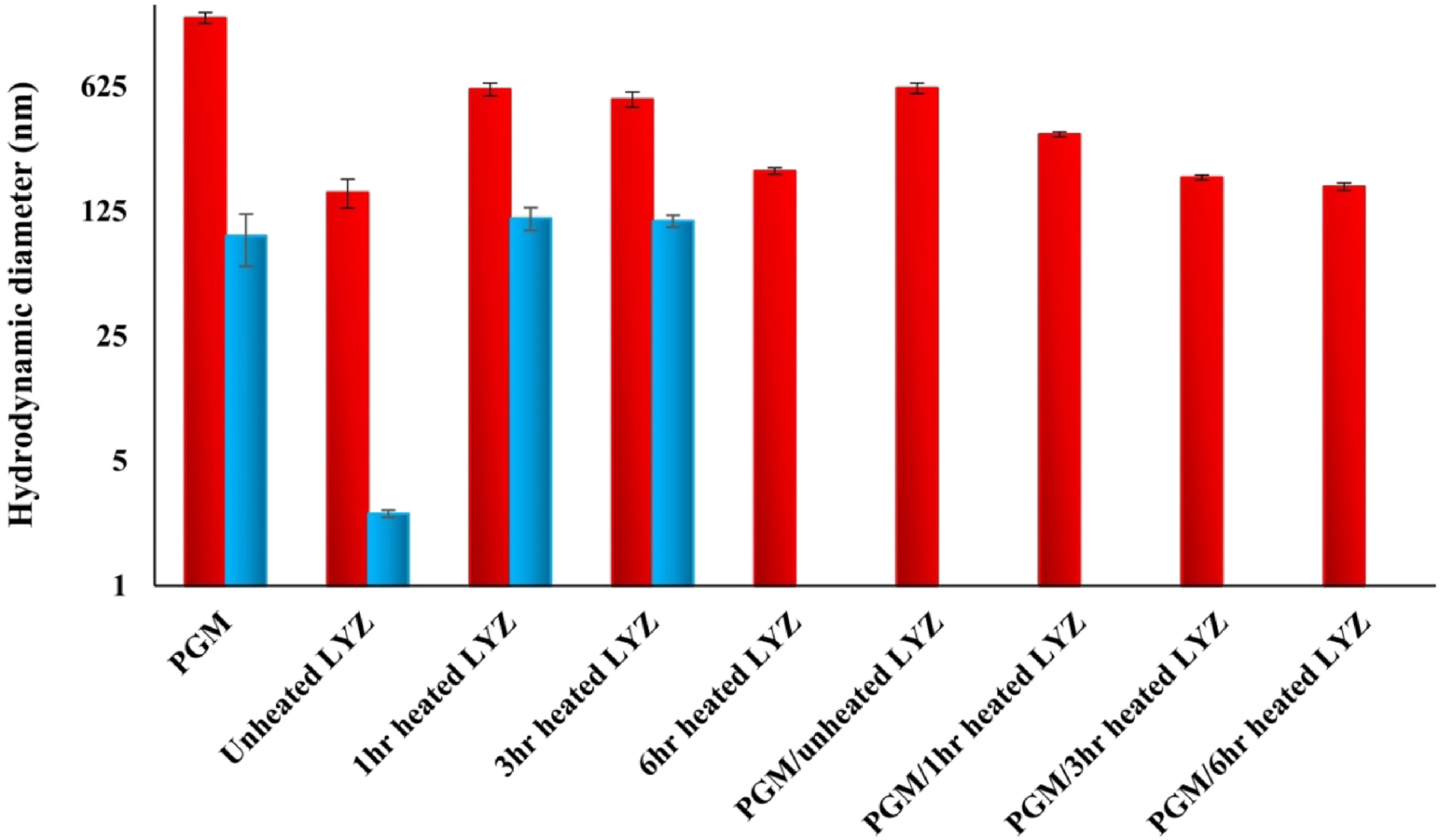
Hydrodynamic diameter (nm)
625
125
25
5
1
PGM
Unheated LYZ
1hr heated LYZ
3hr heated LYZ
6hr heated LYZ
PGM/unheated LYZ
PGM/1hr heated LYZ
PGM/3hr heated LYZ
PGM/6hr heated LYZ

Figure 5

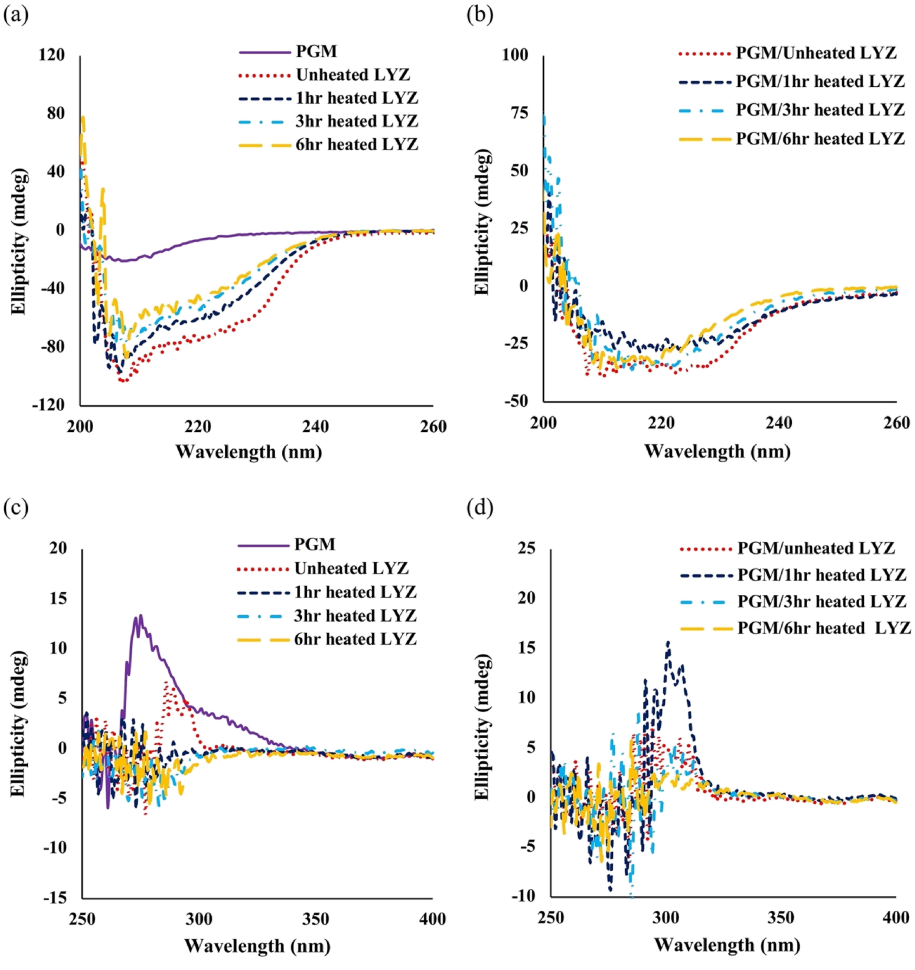
(a)
PGM
Unheated LYZ
1hr heated LYZ
3hr heated LYZ
6hr heated LYZ
Ellipticity (mdeg)
Wavelength (nm)
(b)
PGM/Unheated LYZ
PGM/1hr heated LYZ
PGM/3hr heated LYZ
PGM/6hr heated LYZ
Ellipticity (mdeg)
Wavelength (nm)
(c)
PGM
Unheated LYZ
1hr heated LYZ
3hr heated LYZ
6hr heated LYZ
Ellipticity (mdeg)
Wavelength (nm)
(d)
PGM/unheated LYZ
PGM/1hr heated LYZ
PGM/3hr heated LYZ
PGM/6hr heated LYZ
Ellipticity (mdeg)
Wavelength (nm)

Figure 6

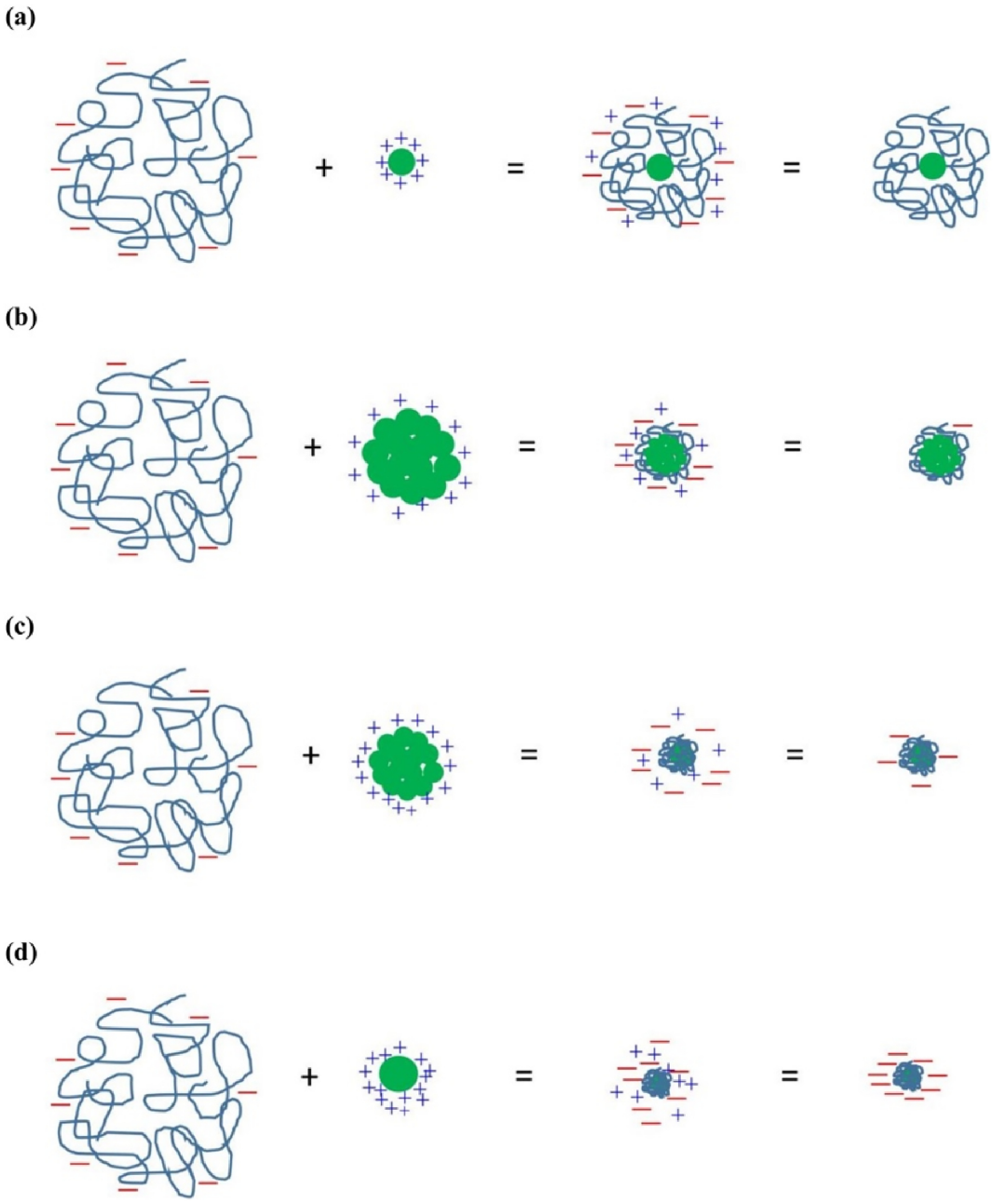


Figure 7